

A preconditioning approach for improved estimation of sparse polynomial chaos expansions

Negin Alemazkoo, Hadi Meidani

Department of Civil and Environmental Engineering, University of Illinois at Urbana-Champaign, Urbana, Illinois, USA.

Abstract

Compressive sampling has been widely used for sparse polynomial chaos (PC) approximation of stochastic functions. The recovery accuracy of compressive sampling highly depends on the incoherence properties of the measurement matrix. In this paper, we consider preconditioning the underdetermined system of equations that is to be solved. Premultiplying a linear equation system by a non-singular matrix results in an equivalent equation system, but it can potentially improve the incoherence properties of the resulting preconditioned measurement matrix and lead to a better recovery accuracy. When measurements are noisy, however, preconditioning can also potentially result in a worse signal-to-noise ratio, thereby deteriorating recovery accuracy. In this work, we propose a preconditioning scheme that improves the incoherence properties of measurement matrix and at the same time prevents undesirable deterioration of signal-to-noise ratio. We provide theoretical motivations and numerical examples that demonstrate the promise of the proposed approach in improving the accuracy of estimated polynomial chaos expansions.

1. Introduction

Reliable analysis of natural and engineered systems necessitates the understanding of how the system response or quantity of interest (QoI) depends on uncertain inputs. Uncertainty quantification (UQ) tackles these issues with efficient propagation of input uncertainties onto the QoI. This is typically done by building approximate surrogates that replace computationally expensive simulations. Surrogates approximate QoI as an analytical function of random inputs and facilitate quantifying parametric uncertainty. As a widely used spectral surrogate, the polynomial chaos expansion (PCE) uses orthogonal polynomials for the approximation of QoI. In order to construct PCEs, i.e., to determine the expansion coefficients corresponding to different polynomial bases, a widely used approach is stochastic collocation. This approach is advantageous particularly because it is nonintrusive and easy to implement by reusing legacy codes. Examples of stochastic collocation methods include spectral projection [1, 2], sparse grid interpolation [3, 4], and least square [5, 6]. The outstanding challenge is that the number of sample points, e.g. sampled simulations, that these methods require for accurate prediction increases drastically as the number of uncertain inputs, or the dimension of the PCE, increases.

Recently, motivated by the fact that approximated PCEs for many high dimensional problems could be sparse, compressive sampling has been effectively used to approximate PCE coefficients using a small number of sampled simulations and has thus alleviated the dimensionality-related challenge [7, 8, 9, 10, 11, 12]. The accuracy of sparse polynomial approximation heavily relies on incoherence properties of measurement matrix, which is a matrix that consists of evaluated polynomial bases at sample points. Most commonly, in standard sampling, samples are generated randomly from the probability distribution of random inputs. Recently, other sampling strategies have been proposed in order to improve the accuracy of sparse PCEs. In [13], it was proposed to draw samples from Chebyshev probability distribution to construct a sparse Legendre-based PCE. The theoretical and numerical results in [9] showed that Chebyshev sampling deteriorates the recovery accuracy in high dimensional problems. Drawing samples randomly from the tensor grid of Gaussian quadrature points was recommended in [8, 14]. Although the results showed significant accuracy improvement in low-dimensional problems, the results underperformed or were close to standard sampling in high-dimensional problems. A sampling strategy that outperforms standard sampling in both low-dimensional high-order and high-dimensional low-order problems was proposed in [15], and was called the coherence-optimal sampling. In coherence-optimal sampling, samples are drawn from a measure that minimizes the (local) coherence of orthogonal polynomial system. In [10], a near-optimal sampling strategy

was proposed, which further improved coherence-optimal sampling by subsampling a few samples from a large pool of coherence-optimal samples in such a way that the resulting measurement matrix will have better cross-correlation properties.

In this work, instead of relying on experimenting with sampling strategies to improve incoherence properties, we take an alternative approach and use a preconditioning scheme to enhance these properties. The term *preconditioning* has already been used in the sparse PCE literature to refer to a weight matrix that is added to preserve asymptotic orthogonality of basis functions when non-standard sampling distributions are used [16, 15]. In underdetermined cases where a limited set of samples are available, enforcing asymptotic orthogonality does not necessarily guarantee improvement in incoherence properties of actual measurement matrices.

To the best of our knowledge, our present work is the first attempt at preconditioning the underdetermined measurement matrix towards better incoherence properties for polynomial chaos approximation. When the target stochastic function is exactly sparse with respect to the truncated PC bases and measurements are noiseless, one can borrow methods for designing optimal projection (or sensing) matrix in signal processing applications [17, 18] to precondition underdetermined equation systems. This is because both the preconditioning matrix and the projection matrix will appear in the same way in the coherence-based objective that one seeks to optimize. However, when modeling or truncation error or measurement noise is present, that resemblance no longer exists. Therefore, in these polynomial regression problems, an improper design of preconditioning matrix can undesirably amplify the noise vector more than it does the measurement vector. This can result in a worse "signal-to-noise" ratio leading to inaccurate polynomial approximation.

In this work, we propose an original approach for designing the preconditioning matrix such that (1) the incoherence properties of the resulting preconditioned measurement matrix are improved, and (2) undesirable amplification of noise vector vis-à-vis measurement vector is prevented. The proposed preconditioning technique is also capable of preconditioning a system with no measurement or truncation error, and as such has general applicability. Using numerical examples, it will be demonstrated that preconditioning can significantly improve the accuracy of PCE surrogates built using compressive sampling. This paper is organized as follows: Section 2 provides a brief overview on application of compressive sampling in PCE approximation; Section 3 introduces the preconditioning scheme along with the theoretical motivation, and Section 4 includes numerical illustration and detailed discussion about the comparative performance of the proposed preconditioning scheme.

2. Setup and background

2.1. Polynomial chaos expansion

Consider the vector of independent random variables $\Xi = (\Xi_1, \dots, \Xi_d)$ to be d -dimensional system random inputs and $u(\Xi)$ to be the uncertain QoI with finite variance. Then, $u(\Xi)$ can be written as an expansion of orthogonal polynomials, i.e.

$$u(\Xi) = \sum_{\alpha \in \mathbb{N}_0^d} c_\alpha \psi_\alpha(\Xi). \quad (1)$$

Let $I_\Xi \subseteq \mathbb{R}^d$ be a tensor-product domain that is the support of Ξ , i.e. $\Xi_i \in I_{\Xi_i}$ and $I_\Xi = \times_{i=1}^d I_{\Xi_i}$. Also, let $\rho_i : I_{\Xi_i} \rightarrow \mathbb{R}^+$ be the probability measure for variable Ξ_i and let $\rho(\Xi) = \prod_{i=1}^d \rho_i(\Xi_i)$. Given this setting, the set of univariate orthonormal polynomials, $\{\psi_{\alpha,i}\}_{\alpha \in \mathbb{N}_0}$, satisfies

$$\int_{I_{\Xi_i}} \psi_{n,i}(\xi_i) \psi_{m,i}(\xi_i) \rho_i(\xi_i) d\xi_i = \delta_{mn}, \quad m, n \in \mathbb{N}_0. \quad (2)$$

Consequently, the d -dimensional orthonormal polynomials $\{\psi_\alpha\}_{\alpha \in \mathbb{N}_0^d}$ in Ξ are formed by the product of the univariate orthonormal polynomials,

$$\psi_\alpha(\Xi) = \prod_{i=1}^d \psi_{\alpha_i,i}(\Xi_i), \quad (3)$$

where α_i represents the i th coordinate of α . For practicality, we need to truncate the expansion in (1) by limiting the total order of polynomial to be k and only including bases with $\|\alpha\|_1 \leq k$ in the expansion. The

cardinality of basis set, denoted by K , will then be

$$K := \frac{(k+d)!}{k! d!}. \quad (4)$$

The resulting truncated PCE, $u_k(\Xi)$, offers a practical approximation of $u(\Xi)$ (inducing a truncation error),

$$u(\Xi) \approx u_k(\Xi) := \sum_{\|\alpha\|_1 \leq k} c_\alpha \psi_\alpha(\Xi). \quad (5)$$

The exact PCE coefficients in Equation 1 can be exactly calculated by projecting $u(\Xi)$ onto the basis functions ψ_α :

$$c_\alpha = \mathbb{E}_\rho [u(\Xi) \psi_\alpha(\Xi)] = \int_{I_\Xi} u(\xi) \psi_\alpha(\xi) \rho(\xi) d\xi. \quad (6)$$

In the typical absence of analytical solution for this multidimensional integral, the PCE coefficients can be numerically calculated using non-intrusive approaches such as Monte Carlo sampling and sparse grid quadrature [19]. However, it is known that Monte Carlo sampling converges slowly and sparse grid quadrature can be impractical in high-dimensional problems [19, 20]. In practice, for high-dimensional problems, least squares regression is widely used for the calculation of PCE coefficients. This approach requires the number of samples to be larger than the number of unknown coefficients, in order to make the system of equations overdetermined. The generally accepted oversampling rate is about 1.5 to 3 times the number of coefficients [21, 5]. Recently, a quasi-optimal sampling approach was introduced in [5] that allows accurate coefficient recovery with $\mathcal{O}(1)$ oversampling rate. However, affording that many samples may still be computationally impossible. In [7] it was shown that when the QoI is sparse with respect to the PCE bases, compressive sampling can be used to calculate the expansion coefficients using samples that are much fewer than the unknown coefficients. This section follows with a brief introduction of compressive sampling application in PCE approximation.

2.2. Sparse PCE estimation via compressive sampling

Compressive sampling first emerged in the field of signal possessing and has since found applications in various domains, such as radar systems [22], speech recognition [23] and MR imaging [24]. Compressive sampling solves an underdetermined system of equations by exploring its sparsest solution. Here, we present the compressive sampling in the context of stochastic collocation. Specifically, consider M realizations $\{\xi^{(i)}\}_{i=1}^M$ of system inputs, with corresponding model outputs $\mathbf{u} = (u(\xi^{(1)}), \dots, u(\xi^{(M)}))^T$. We seek a solution that satisfies

$$\Psi \mathbf{c} = \mathbf{u}, \quad (7)$$

where Ψ is the Vandermonde-like matrix, often referred to as the measurement or design matrix, and is constructed according to

$$\Psi = [\psi_{ij}], \quad \psi_{ij} = \psi_{\alpha^j}(\xi^{(i)}), \quad 1 \leq i \leq M, \quad 1 \leq j \leq K. \quad (8)$$

The problem 7 is underdetermined and ill-posed when $M < K$. Therefore, obtaining a unique solution requires adding regularization to the problem. In compressive sampling, the main goal is to determine the sparsest solution, which can be achieved by minimizing the ℓ_0 -norm of the solution according to

$$\min_{\mathbf{c}} \|\mathbf{c}\|_0 \quad \text{subject to} \quad \Psi \mathbf{c} = \mathbf{u}. \quad (9)$$

However, since the ℓ_0 -norm is non-convex and discontinuous, the above problem is NP-hard. Therefore, ℓ_0 minimization is usually replaced with its convex relaxation, where the ℓ_1 -norm of the solution \mathbf{c} is minimized instead, i.e.,

$$\min_{\mathbf{c}} \|\mathbf{c}\|_1 \quad \text{subject to} \quad \Psi \mathbf{c} = \mathbf{u}. \quad (10)$$

Under certain conditions, ℓ_1 minimization gives the same solution as ℓ_0 minimization [25]. The ℓ_1 minimization problem is commonly known as the *Basis Pursuit*. In case of noisy measurements or when $u(\Xi)$ can not be exactly represented by k th order PC basis, one can use the *Basis Pursuit Denoising* [26] formulated as

$$\min_{\mathbf{c}} \|\mathbf{c}\|_1 \quad \text{subject to} \quad \|\Psi \mathbf{c} - \mathbf{u}\|_2 \leq \epsilon, \quad (11)$$

where ϵ is the error tolerance. Other types of regularizations such as *Least Absolute Shrinkage and Selection Operator (lasso)*, ℓ_{1-2} minimization and $\ell_{0.5}$ regularization can also be used [27, 28, 29, 30].

2.3. ℓ_1 minimization recoverability

The ability of ℓ_1 minimization in accurate solution recovery depends on the actual sparsity of the solution \mathbf{c} and properties of the measurement matrix Ψ . Here, we discuss one of the main properties of Ψ , shown to be significantly relevant to recovery accuracy.

Definition 1. (restricted isometry constant [31]) *The s -restricted isometry constant for a matrix $\Psi \in \mathbb{R}^{M \times K}$ is defined to be the smallest $\delta_s \in (0, 1)$ such that*

$$(1 - \delta_s) \|\mathbf{c}\|_2^2 \leq \|\Psi \mathbf{c}\|_2^2 \leq (1 + \delta_s) \|\mathbf{c}\|_2^2, \quad (12)$$

for all $\mathbf{c} \in \mathbb{R}^K$ that are at most s -sparse.

Depending on the property of this isometry constant, one can expect the ℓ_1 minimization (10) to produce a very accurate and even exact solution, as stated in the following theorem.

Theorem 1 ([31]). *Let $\Psi \in \mathbb{R}^{M \times K}$ with isometry constant δ_{2s} such that $\delta_{2s} < \sqrt{2} - 1$. For a given $\bar{\mathbf{c}}$, and measurement $\mathbf{y} = \Psi \bar{\mathbf{c}}$, let \mathbf{c} be the solution of*

$$\min \|\mathbf{c}\|_1 \quad \text{subject to} \quad \Psi \mathbf{c} = \mathbf{y}. \quad (13)$$

Then the reconstruction error satisfies

$$\|\mathbf{c} - \bar{\mathbf{c}}\| \leq C_1 \frac{\|\bar{\mathbf{c}} - \mathbf{c}^*\|}{\sqrt{s}} \quad (14)$$

where C_1 only depends on δ_{2s} and \mathbf{c}^* is the vector $\bar{\mathbf{c}}$ with all but the s -largest entries set to be zero. If $\bar{\mathbf{c}}$ is s -sparse, then the recovery is exact.

Since calculating the isometry constant is an NP-complete problem, one can use the following theorem which provides a probabilistic upper bound on the isometry constant for bounded orthonormal systems. An orthonormal system $\{\psi_n\}_{1 \leq n \leq K}$ with respect to density $\rho(\xi)$ is a bounded orthonormal system if it satisfies

$$\sup_{1 \leq n \leq K} \|\psi_n\|_\infty = \sup_{1 \leq n \leq K} \sup_{\xi \in \text{supp}(\rho)} |\psi_n(\xi)| \leq L. \quad (15)$$

Theorem 2 ([32]). *Let $\{\psi_n\}_{1 \leq n \leq K}$ be a bounded orthonormal system. Also let $\Psi \in \mathbb{R}^{M \times K}$ be a measurement matrix with entries $\{\psi_{ij} = \psi_j(\xi^{(i)})\}_{1 \leq i \leq M, 1 \leq j \leq K}$, where $\xi^{(1)}, \dots, \xi^{(M)}$ are random samples drawn from measure ρ . Assuming that*

$$M \geq C \delta^{-2} L^2 s \log^3(s) \log(K), \quad (16)$$

then with probability at least $1 - K^{-\beta \log^3(s)}$, the isometry constant δ_s of $\frac{1}{\sqrt{M}} \Psi$ satisfies $\delta_s \leq \delta$. $C, \beta > 0$ are universal constants.

It should be noted that L is the smallest such constant for which inequality 15 holds. Hereinafter, let us refer to bound L as the local-coherence.

2.4. Enhanced sampling strategies

Theorem 2 has motivated new sampling approaches, including coherence-optimal sampling introduced in [15]. In this approach, instead of directly sampling from the probability measure, $\rho(\xi)$, samples are drawn from a different optimal probability measure, $\rho_o(\xi)$, which was shown to result in the lowest local-coherence. The optimal measure $\rho_o(\xi)$ is constructed according to

$$\rho_o(\xi) = C^2 \rho(\xi) B^2(\xi), \quad (17)$$

where C is a normalizing constant and

$$B(\xi) := \max_{\|\alpha\|_1 \leq k} |\psi_\alpha(\xi)|. \quad (18)$$

Corresponding to this new probability measure, a weight function should be used to maintain asymptotic orthogonality between the polynomial bases. This weight function is given by

$$w(\boldsymbol{\xi}) = \frac{1}{B(\boldsymbol{\xi})}. \quad (19)$$

Accordingly, the following weighted ℓ_1 -minimization is solved for sparse recovery

$$\min_{\mathbf{c}} \|\mathbf{c}\|_1 \quad \text{subject to} \quad \|\mathbf{W}\boldsymbol{\Psi}\mathbf{c} - \mathbf{W}\mathbf{u}\|_2 \leq \epsilon, \quad (20)$$

where \mathbf{W} is the $M \times M$ diagonal weight matrix, with $\mathbf{W}(i, i) = w(\boldsymbol{\xi}^{(i)})$ for $i = 1, \dots, M$.

It has been shown that coherence-optimal sampling can significantly improve the accuracy of sparse recovery for PCE [15]. In [10], a near-optimal sampling approach was proposed, which aimed to simultaneously improve the local-coherence and the cross-correlation properties of the resulting measurement matrix. In this approach, first a large pool of sample candidates are drawn from the coherence-optimal sampling distribution, out of which the final sample set of size M is selected such that the cross-correlation properties of the resulting measurement matrix are improved. Numerical examples have shown that near-optimal sampling can significantly improve the accuracy of sparse PCE recovery for system responses with various combinations of dimensionality and order.

In this work, we introduce an alternative preconditioning approach for improving the properties of measurement matrix. This approach can particularly address the case where samples have already been drawn using expensive simulations or costly experiments and sampling strategies have become inapplicable. Next section introduces our proposed design approach for the preconditioning matrix.

3. A preconditioning scheme

In Sections 2.2, we discussed the relevant properties of the measurement matrix $\boldsymbol{\Psi}$ that can impact the recovery accuracy, and discussed how one can enhance the recovery accuracy using advanced sampling strategies [15, 14, 10]. However, when the sample points are already obtained, the only way to improve the properties of $\boldsymbol{\Psi}$ is through preconditioning. To this end, one can multiply the measurement matrix with a preconditioning matrix, $\mathbf{P} \in \mathbb{R}^{M \times M}$, such that the preconditioned measurement matrix $\mathbf{P}\boldsymbol{\Psi}$ is less coherent than the original measurement matrix. One can then solve the following ℓ_1 -minimization

$$\min_{\mathbf{c}} \|\mathbf{c}\|_1 \quad \text{subject to} \quad \|\mathbf{P}\boldsymbol{\Psi}\mathbf{c} - \mathbf{P}\mathbf{u}\|_1 \leq \epsilon. \quad (21)$$

The weight matrix in (20) can be thought of as a preconditioning matrix, which improves the properties of the measurement matrix. However, by definition it is a diagonal matrix, with its diagonal terms $w(i, i)$ being a function of the i th sample location. Here, we do not force \mathbf{P} to be diagonal, neither do we constrain it to be a function of sample locations. In what follows, we discuss the relevant criteria used in our design of preconditioning matrix.

Let us first define $\mathbf{D} \triangleq \mathbf{P}\boldsymbol{\Psi} \in \mathbb{R}^{M \times K}$ and call it the *equivalent measurement matrix*. One of the main properties of \mathbf{D} that directly impacts the recovery accuracy is its spark. The spark of a matrix is the smallest number of its columns that are linearly dependent. It is known that ℓ_1 minimization is guaranteed to recover an s -sparse signal vector if $\text{spark}(\mathbf{D}) > 2s$. Designing the preconditioning matrix such that the spark of the equivalent measurement matrix is maximized would allow the exact recovery of a larger set of signals. However, computing the spark of a matrix is an NP-hard problem. Alternatively, one can analyze recovery guarantees using other properties which are easier to compute. One such property is the mutual-coherence, which for a given matrix is defined as the maximum absolute normalized inner product, i.e. the cross-correlation, between its columns [7, 33]. Let $D_1, D_2, \dots, D_K \in \mathbb{R}^M$ be the columns of matrix \mathbf{D} . The mutual-coherence of matrix \mathbf{D} , denoted by $\mu(\mathbf{D})$, is then given by

$$\mu(\mathbf{D}) := \max_{1 \leq i, j \leq K, i \neq j} \frac{|D_j^T D_i|}{\|D_j\|_2 \|D_i\|_2}. \quad (22)$$

Mutual-coherence gives a lower bound for spark as follows [34]

$$\text{spark}(\mathbf{D}) \geq 1 + \frac{1}{\mu(\mathbf{D})}. \quad (23)$$

It may be concluded that preconditioning matrix \mathbf{P} should be designed in a way that mutual-coherence of \mathbf{D} is minimized. However, it has been observed that minimizing mutual-coherence does not necessarily improve the recovery accuracy of compressive sampling [18, 35]. This is because mutual coherence only serves as a lower bound on the spark, and minimizing mutual-coherence is optimizing only for the worst-case scenario and fails to reflect upon other possibilities for improving compressive sampling performance [35].

Theorem 2 suggests that optimizing the preconditioning matrix so that isometry constant of the equivalent measurement matrix is minimized will be effective. However, as previously mentioned, calculating isometry constant for a given matrix is an NP-complete problem. If one considers all the column-submatrices of the equivalent measurement matrix that has $s^* \leq s$ columns, it is known that the eigenvalues of these column-submatrices are bounded by the isometry constant. Therefore, one may suggest to minimize the condition number of all column-submatrices with s or fewer columns. However, calculating such combinatorial measure is not a trivial task either and can be computationally impossible [35].

As a result, establishing a single matrix property that (i) is directly associated with the accuracy of the compressive sampling method and (ii) is easily computable still remains an open challenge [18, 35]. To sidestep this challenge, efforts have focused on identifying properties or measures that are relatively better than the mutual-coherence. For example, the average coherence of the equivalent measurement matrix can be minimized [35]. Alternatively, one can minimize the distance between the Gram matrix, $\mathbf{D}^T \mathbf{D}$, and the identity matrix or an equiangular tight frame (ETF) Gram matrix [18, 17, 36, 37]. ETF matrices are matrices consisting of unit vectors whose maximum cross-correlation achieves the smallest possible value, and as such are ideal measurement matrices for sparse recovery.

When $\mathbf{\Psi} \mathbf{c} + \mathbf{e} = \mathbf{u}$, where \mathbf{e} is the vector representing noise and/or modeling error, a preconditioning matrix obtained by minimizing the distance between Gram matrix and ETF Gram matrix may magnify the noise while reducing the magnitude of observation vector. In other words, it's possible that $\|\mathbf{P}\mathbf{e}\|_2$ is large while $\|\mathbf{P}\mathbf{u}\|_2$ is relatively small when \mathbf{P} is not properly chosen, thereby deteriorating the signal-to-noise ratio and in turn the PCE approximation accuracy.

Similar issue exists for designing a projection (or sensing) matrix in signal processing application. Recent studies have proposed to design a projection matrix such that it improves incoherence properties of equivalent dictionary, and its multiplication by the noise vector results in a vector with small magnitude [38, 39, 40]. However, it's more challenging to design a preconditioning matrix for an underdetermined regression problem as both sides of the equation, $\mathbf{\Psi} \mathbf{c} + \mathbf{e} = \mathbf{u}$, are multiplied by the preconditioning matrix. Therefore, designing a preconditioner such that $\|\mathbf{P}\mathbf{e}\|_2$ is minimized may result in undesirably small magnitude for $\|\mathbf{P}\mathbf{u}\|_2$.

Alternatively, one may propose designing the preconditioning matrix such that $\|\mathbf{P}\mathbf{u}\|_2$ is maximized. However, this doesn't provide control over how much the noise vector gets magnified. To prevent undesirable relative magnification for $\|\mathbf{P}\mathbf{e}\|_2$ and $\|\mathbf{P}\mathbf{u}\|_2$, we seek to design a preconditioning matrix that (1) results in a small distance between the Gram matrix and the ETF Gram matrix and (2) is not too much different from the identity matrix. We choose identity matrix since it is guaranteed not to disproportionately magnify the noise vector as compared with the measurement vector. The choice of identity matrix as a reference matrix is robust in the sense that it does not assume any particular choice for the measurement noise distribution. Following these reasonings, we form the following problem for the design of preconditioning matrix:

$$\min_{\mathbf{P} \in \mathbb{R}^{M \times M}, \mathbf{G} \in H_{\mu_E}} f(\mathbf{G}, \mathbf{P}) = \|\mathbf{G} - \mathbf{\Psi}^T \mathbf{P}^T \mathbf{P} \mathbf{\Psi}\|_F + \lambda \|\mathbf{I} - \mathbf{P}\|_F, \quad (24)$$

where $\|\cdot\|_F$ denotes the Frobenius norm and \mathbf{G} is the targeted ETF Gram matrix which belongs to the space

$$H_{\mu_E} = \left\{ \mathbf{G} \in \mathbb{R}^{K \times K} : \mathbf{G} = \mathbf{G}^T, G_{ii} = 1, \max_{i \neq j} |G_{ij}| < \mu_E \right\}, \quad (25)$$

where μ_E is the lower bound for the mutual-coherence of matrix $\mathbf{\Psi}$ of dimension $M \times K$ given by

$$\mu_E := \sqrt{\frac{K - M}{M(K - 1)}}. \quad (26)$$

When $\lambda = 0$, the problem defined in (24) is usually solved using alternating minimization method, where \mathbf{P} is updated using a gradient-based algorithm [17, 38]. Here, we use the similar approach to solve 24 with $\lambda > 0$. The gradient of $f(\mathbf{G}, \mathbf{P})$ with respect to \mathbf{P} is given by

$$\frac{\partial f}{\partial \mathbf{P}} = \frac{\partial}{\partial \mathbf{P}} \text{Tr} \{ (\mathbf{G} - \Psi^T \mathbf{P}^T \mathbf{P} \Psi)^T (\mathbf{G} - \Psi^T \mathbf{P}^T \mathbf{P} \Psi) \} + \lambda \frac{\partial}{\partial \mathbf{P}} \text{Tr} \{ (\mathbf{I} - \mathbf{P})^T (\mathbf{I} - \mathbf{P}) \}, \quad (27)$$

where $\text{Tr} \{ \cdot \}$ denotes the trace operator. Using matrix derivative rules, Equation 27 can be further simplified to

$$\frac{\partial f}{\partial \mathbf{P}} = 4\mathbf{P}\Psi(\Psi^T \mathbf{P}^T \mathbf{P} \Psi - \mathbf{G})\Psi^T + 2\lambda(\mathbf{P} - \mathbf{I}). \quad (28)$$

Given the gradient of $f(\mathbf{G}, \mathbf{P})$, the conjugate gradient method is used to solve 24 for a fixed \mathbf{G} . We then use an alternating approach to solve (24). Our alternating approach keeps one of the two variables in 24 constant and solves the problem by varying the other parameter. When \mathbf{G} is fixed, as we explained, the conjugate gradient method is used to evaluate the solution of 24. Once \mathbf{P} is fixed, the optimal \mathbf{G} can be simply obtained by projecting the Gram matrix of column-normalized equivalent measurement matrix, $\tilde{\mathbf{D}}$, onto the set H_{μ_E} [17] according to:

$$G_{ij} = \begin{cases} 1, & i = j, \\ \tilde{G}_{ij}, & i \neq j, |\tilde{G}_{ij}| \leq \mu_E, \\ \text{sign}(\tilde{G}_{ij}) \cdot \mu_E, & i \neq j, |\tilde{G}_{ij}| > \mu_E, \end{cases} \quad (29)$$

where $\text{sign}(\cdot)$ is a sign function, and $\tilde{\mathbf{G}} = \tilde{\mathbf{D}}^T \tilde{\mathbf{D}}$. Algorithm 1 shows the alternating approach to solve 24.

Algorithm 1 The alternating solution for minimization problem 24

- 1: Initialization: Set a convergence threshold δ_{thr} ; set \mathbf{P}_0 to be a random matrix, and \mathbf{G}_0 to be the identity matrix.
 - 2: **while** $\delta_t < \delta_{\text{thr}}$ **do**
 - 3: Form equivalent measurement matrix: $\mathbf{D} = \mathbf{P}_{t-1} \Psi$.
 - 4: Form column-normalized equivalent measurement matrix: $\tilde{\mathbf{D}}$.
 - 5: $\tilde{\mathbf{G}} = \tilde{\mathbf{D}}^T \tilde{\mathbf{D}}$.
 - 6: $G_t(i, j) = \begin{cases} 1, & i = j, \\ \tilde{G}_{ij}, & i \neq j, |\tilde{G}_{ij}| \leq \mu_E, \\ \text{sign}(\tilde{G}_{ij}) \cdot \mu_E, & i \neq j, |\tilde{G}_{ij}| > \mu_E. \end{cases}$
 - 7: Solve $\mathbf{P}_t = \underset{\mathbf{P} \in \mathbb{R}^{M \times M}}{\text{argmin}} f(\mathbf{G}_t, \mathbf{P})$ using conjugate gradient method.
 - 8: $\delta_t = [f(\mathbf{G}_t, \mathbf{P}_t) - f(\mathbf{G}_{t-1}, \mathbf{P}_{t-1})] / f(\mathbf{G}_{t-1}, \mathbf{P}_{t-1})$.
 - 9: **end while**
-

Algorithm 1 is used to solve 24 for a fixed λ value. We propose a cross-validation approach that identifies the λ value that results in best PC approximation accuracy. To do so we first randomly divide the M samples into M_{tr} training samples and M_{val} validation samples. Then, for each λ value, using all the M samples, we design a preconditioning matrix which leads to an equivalent measurement matrix $\mathbf{P}\Psi$. We then select M_{tr} rows of this measurement matrix, based on the training samples, to form the training submatrix of size $M_{\text{tr}} \times K$. Using this training measurement submatrix we estimate the expansion coefficients and calculate the validation error over the validation samples. Once this is done for all the choices of λ values, we then choose the λ value and its associated preconditioning matrix that results in the smallest validation error. Algorithm 2 shows the steps for the proposed cross-validation algorithm. In this pseudo-code, superscripts ‘tr’ and ‘val’ denote the row-submatrices associated with training and validation samples, respectively.

Algorithm 2 Cross-validation algorithm for weigh parameter λ

- 1: Initialization: Form a set of N candidate values for λ : $\{\lambda_1, \dots, \lambda_N\}$.
 - 2: Randomly divide the available M samples into M_{tr} training samples and M_{val} validation samples.
 - 3: **for** $i = 1 : N$ **do**
 - 4: Solve $\mathbf{P}_i = \underset{\mathbf{P} \in \mathbb{R}^{M \times M}, \mathbf{G} \in H_{\mu_E}}{\text{argmin}} \left\| \mathbf{G} - \mathbf{\Psi}^T \mathbf{P}^T \mathbf{P} \mathbf{\Psi} \right\|_F + \lambda_i \left\| \mathbf{I} - \mathbf{P} \right\|_F$. ▷ Use Algorithm 1
 - 5: Precondition the problem: $\mathbf{D}_i = \mathbf{P}_i \mathbf{\Psi}$ and $\mathbf{u}_{\mathbf{P}_i} = \mathbf{P}_i \mathbf{u}$.
 - 6: Form measurement submatrix \mathbf{D}_i^{tr} and preconditioned measurement subset $\mathbf{u}_{\mathbf{P}_i}^{\text{tr}}$ at training samples.
 - 7: Solve $\mathbf{c}_i = \underset{\mathbf{c}}{\text{argmin}} \left\| \mathbf{c} \right\|_1$ s.t. $\left\| \mathbf{D}_i^{\text{tr}} \mathbf{c} - \mathbf{u}_{\mathbf{P}_i}^{\text{tr}} \right\|_2 \leq \epsilon_i$, ▷ Choose ϵ_i using separate cross-validation
 - 8: Calculate cross-validation error $e_i^{\text{CV}} = \left\| \mathbf{\Psi}^{\text{val}} \mathbf{c}_i - \mathbf{u}^{\text{val}} \right\|_2$.
 - 9: **end for**
 - 10: Choose λ_i that results in the smallest cross-validation error e_i^{CV} .
-

When it is not possible to select a preconditioning matrix without undesirably magnifying the noise, Algorithm 2 will identify a large value for λ , thereby selecting a preconditioning matrix close to an identity matrix. Therefore, it can be argued that the proposed preconditioning approach is expected to either improve or in the worst case preserve the approximation accuracy. In what follows, using numerical examples, we demonstrate the potential accuracy improvement that can be achieved by proposed preconditioning algorithm.

4. Numerical illustration

To demonstrate the improvement in approximation accuracy using the proposed preconditioning scheme, we first conduct a rather comprehensive numerical study and report phase transition diagrams for Hermite- and Legendre-based target functions with different combinations of polynomial dimension, d , and polynomial order, k . As additional numerical examples, we also consider three different types of target functions: (i) functions that are exactly sparse with respect to PC bases together with noiseless measurements, (ii) functions that are approximately sparse with respect to PC bases together with noiseless measurements, and (iii) functions that are exactly sparse with respect to PC bases together with noisy measurements.

In all the examples, we column-normalize the measurement matrix to prevent ℓ_1 minimization biasing towards columns with large norms. Optimization problems (11) and (21) are solved using the SPGL1 package [41]. We use the default setting of SPGL1 package, except for the maximum number of iteration, tolerance for identifying a basis pursuit solution, `bpTol`, and optimality tolerance, `optTol`. We set maximum number of iterations, `bpTol`, and `optTol`, respectively equal to $50M$ (with M being the number of samples), 10^{-8} , and 10^{-6} . The conjugate gradient-based *MinFunc* toolbox [42] is used to solve (24). In Algorithm 1, we set the convergence threshold to be 10^{-2} . Finally, for the cross validation algorithm for λ value, three fourths of the samples are used for training and the rest for validation.

4.1. Phase transition diagrams

As the first illustration case, consider the target function to be in fact a polynomial expansion, i.e. $f(\mathbf{\Xi}) = \sum_{j=1}^K \mathbf{c}_{\alpha^j} \mathbf{\Psi}_{\alpha^j}(\mathbf{\Xi})$, where the known coefficient vector \mathbf{c} is exactly s -sparse. Our objective is to evaluate recoverability of \mathbf{c} using only M samples. To perform a comprehensive recoverability evaluation, we consider several scenarios with varying sparsity and sample size. Specifically, let us consider a unit square $[0, 1]^2$, where the x-axis shows undersampling rates, M/K , and the y-axis shows sparsity rates, s/M . This unit square, which constitutes the domain for phase transition diagrams, typically partitions into three regions: (1) a region where the probability of accurate recovery is near one; (2) a region where the probability of accurate recovery is near zero; (3) a narrow transition region [43, 44]. Furthermore, we consider scenarios where order and dimension of polynomial expansion are varied. For each choice of dimension and order, we divide the unit square to a 50×50 grid. At each point in the grid, i.e. for each combination of d, k, s and M , we study the success rate of the ℓ_1 -minimization on 100 “trial” target expansions. Each trial target expansion is created by randomly selecting s coefficients and assigning them to values drawn from a standard normal distribution, while setting the remaining coefficients equal to zero. For each trial target expansion, the recovery is determined to be successful if $\left\| \mathbf{c} - \bar{\mathbf{c}} \right\|_2 / \left\| \bar{\mathbf{c}} \right\|_2 < 10^{-3}$, where $\bar{\mathbf{c}}$ is the coefficient of the target expansion and \mathbf{c} is the solution of the ℓ_1 -minimization. The recovery probability is then defined as the ratio of successful recoveries among all recoveries for the 100 trial target expansions. Finally, the transition diagrams

are created by connecting the points at which the successful recovery probability is estimated to be 50%. In this work, we compare phase transition diagrams for standard and coherence-optimal sampling with and without preconditioning. It should be noted that in generating ‘coherence-optimal’ results (obtained without our preconditioning scheme) we still apply the weight matrix, \mathbf{W} , as in (19) and solve (20). This weight matrix may also be referred to as a preconditioning matrix. However, in this paper, only the results labeled ‘preconditioned’ have been obtained from our proposed preconditioning approach shown in Algorithm 2.

Figure 1 includes the phase transition diagrams for 3 combinations of dimension and order for Legendre polynomial expansions and shows that preconditioning significantly improves the recovery accuracy. In cases where $d \ll k$ or $k \approx d$ preconditioned coherence-optimal sampling outperforms preconditioned standard sampling. This is because coherence-optimal sampling is expected to outperform standard sampling more significantly in these cases. For large values of k coherence-optimal sampling distribution coverages to Chebyshev distribution, which is the optimal sampling distribution as k goes to infinity [16]. As the dimensionality increases and the polynomial order decreases the coherence-optimal sampling distribution becomes similar to uniform distribution. This can be explained by referring to the coherence-optimal distribution given by $\rho_o(\boldsymbol{\xi}) = C^2 \rho(\boldsymbol{\xi}) B^2(\boldsymbol{\xi})$, where C is a normalizing constant and $B(\boldsymbol{\xi})$ is the largest absolute value of all the polynomial basis functions. For Legendre-based expansions, $\rho_o(\boldsymbol{\xi}) \propto B^2(\boldsymbol{\xi})$. For $d \ll k$ or $d \approx k$, this distribution is expected to peak when $\boldsymbol{\xi}$ values in all dimensions are close to the boundary. To explain this, we note that one-dimensional α_i -degree Legendre polynomials reach their maximum absolute values at their support boundaries, and that $B(\xi_i) \leq (2\alpha_i + 1)^{\frac{1}{2}}$ [9]. Therefore, for d -dimensional Legendre polynomials with the multi-index $\boldsymbol{\alpha}$, we have

$$B(\boldsymbol{\xi}) \leq \prod_{i=1}^d (2\alpha_i + 1)^{\frac{1}{2}}. \quad (30)$$

When $d \ll k$, the expansion will include full-dimensional bases (where all the dimensions are present) and therefore $B(\boldsymbol{\xi})$ is peaked when $\boldsymbol{\xi}$ values in all dimensions are close to the boundary. However, when $d \gg k$, the expansion will not include full-dimensional bases; it will have at most k -dimensional bases, and the full-dimensional bound of Equation 30 will never be triggered. As a result, $B(\boldsymbol{\xi})$ is peaked at samples of $\boldsymbol{\xi}$ that have k entries close to the boundary, and the remaining $d - k$ entries can be randomly located anywhere in the parameter space. Consequently, for large values of d and small values of k , $\rho_o(\boldsymbol{\xi})$ becomes similar to uniform distribution and coherence-optimal sampling produces results similar to those obtained by standard sampling.

Figure 2 includes the phase transition diagrams for Hermite polynomial functions considering the same combinations of dimensionality and order. Again, it can be seen that advantage of coherence-optimal sampling over standard sampling disappears when target solutions become higher-dimensional and lower-order. Also, we observe that in all cases preconditioning significantly improves the recovery accuracy.

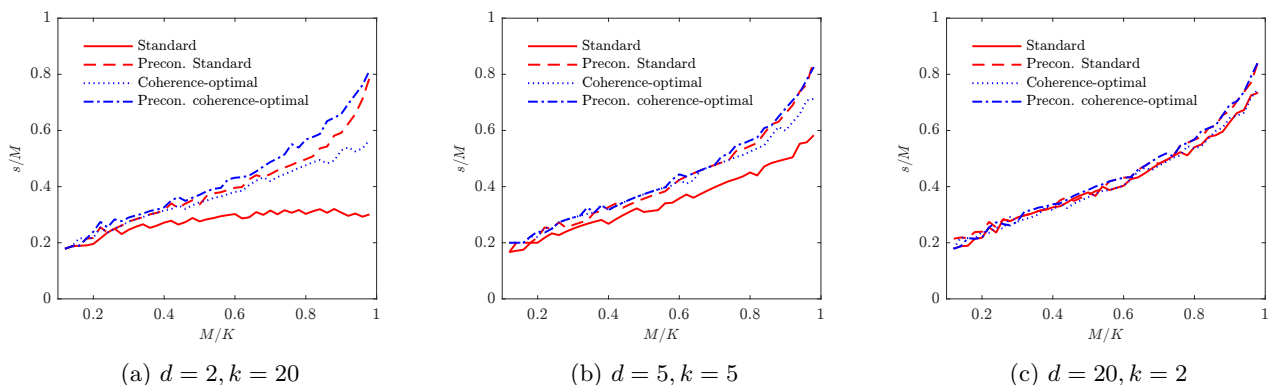


Figure 1: Comparison of phase transition diagrams for standard and coherence-optimal sampling with and without preconditioning for sparse recovery of Legendre-based PCE with three combinations of dimension d and order k .

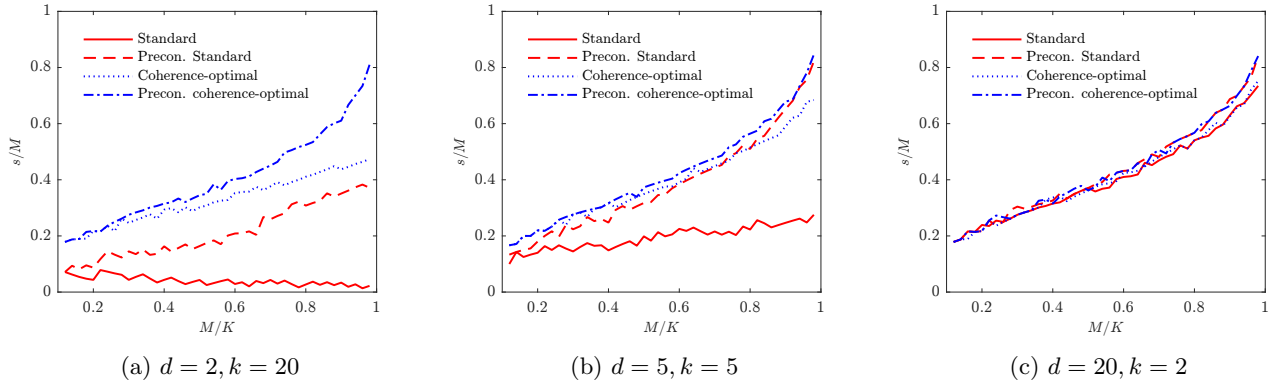


Figure 2: Comparison of phase transition diagrams for standard and coherence-optimal sampling with and without preconditioning for sparse recovery of Hermite-based PCE with three combinations of dimension d and order k .

4.2. Exactly sparse functions

In this section, we consider two functions that are exactly sparse with respects to PC basis. In particular, we consider a low-dimensional high-order and a high-dimensional low-order problem.

4.2.1. A low-dimensional high-order polynomial function

Let $u_1(\Xi)$ to be a sparse 20th-order Hermite polynomial expansion in a two-dimension random space with standard normal distribution, manufactured according to

$$u_1(\Xi) = \sum_{i=1}^9 \Xi_1^i \Xi_2^{i+2}. \quad (31)$$

We aim to recover the sparse vector of coefficients using a smaller set of samples than the cardinality of basis set, which is 231. We compare the approximation accuracy for standard sampling and coherence-optimal sampling with and without preconditioning. For all four approaches, we report the performance results obtained by 100 independent runs, each with an independent set of samples. Figure 3a compares the median, 1st and 3rd quantiles of relative ℓ_2 error with and without preconditioning when standard sampling is used. Relative error is calculated as $\|\mathbf{c} - \bar{\mathbf{c}}\|_2 / \|\bar{\mathbf{c}}\|_2$, where $\bar{\mathbf{c}}$ is the exact coefficient vector and \mathbf{c} is the solution of the associated ℓ_1 minimization. Figure 3b compares the median, 1st and 3rd quantiles of relative ℓ_2 error with and without preconditioning when coherence-optimal sampling is used. As expected, preconditioning improves the approximation accuracy for both standard and coherence-optimal sampling. Also, as it can be concluded from the phase transition diagrams in Figure 2a, the preconditioned coherence-optimal sampling results in the most accurate approximation followed by coherence-optimal and preconditioned standard sampling. It should be noted that coherence-optimal sampling significantly outperforms standard sampling for high-order Hermite polynomials. This explains the outperformance of coherence-optimal sampling over preconditioned standard sampling. Moreover, accuracy improvement achieved by preconditioned coherence-optimal sampling shows that even when samples are drawn from an optimal distribution, accuracy can still be improved using preconditioning.

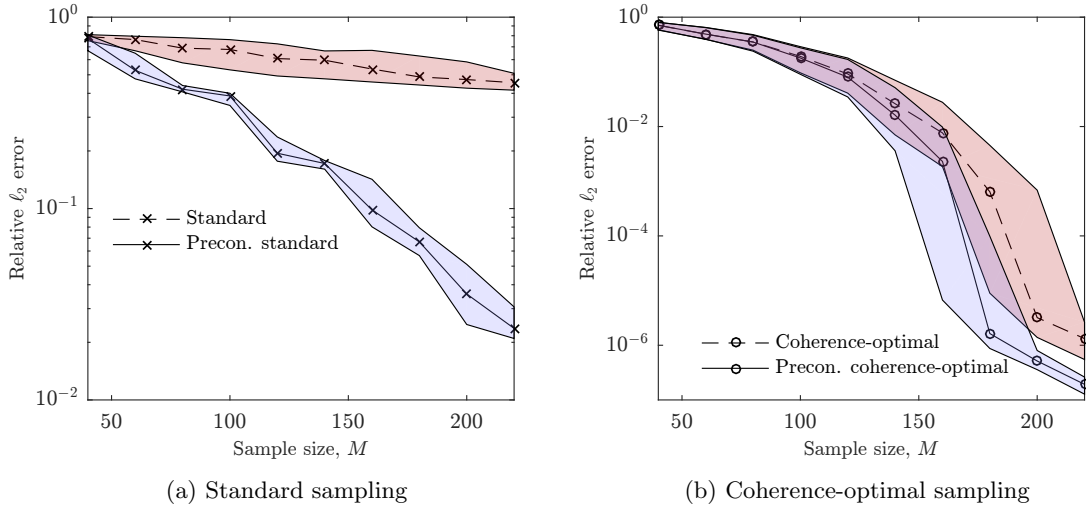


Figure 3: Comparison of relative ℓ_2 error with and without preconditioning for low-dimensional high-order manufactured PCE of Eq. 31 using: (a) standard sampling, (b) coherence-optimal sampling

4.2.2. A high-dimensional low-order polynomial function

As a contrasting example, we consider $u_2(\Xi)$ to be a sparse second-order Legendre polynomial expansion in a 20-dimensional random space with uniform density on $[-1, 1]^{20}$, manufactured according to

$$u_2(\Xi) = \sum_{i=1}^{19} \Xi_i \Xi_{i+1} + \sum_{i=1}^{20} \Xi_i^2. \quad (32)$$

Similar to previous example, the cardinality of basis set is 231 and we aim to recover the vector of coefficients using a small set of samples. To compare the performance of coherence-optimal and standard sampling with and without preconditioning on this target function, the numerical results were obtained under a setting similar to that in the previous example with 100 independent runs for all the four approaches. Figures 4a and 4b compare the median, 1st and 3rd quantiles of relative ℓ_2 error when standard sampling and coherence-optimal sampling is used, respectively. It can be seen that the improvement in approximation accuracy achieved by coherence-optimal sampling, over standard sampling, is insignificant. However, preconditioning successfully improves the approximation accuracy.

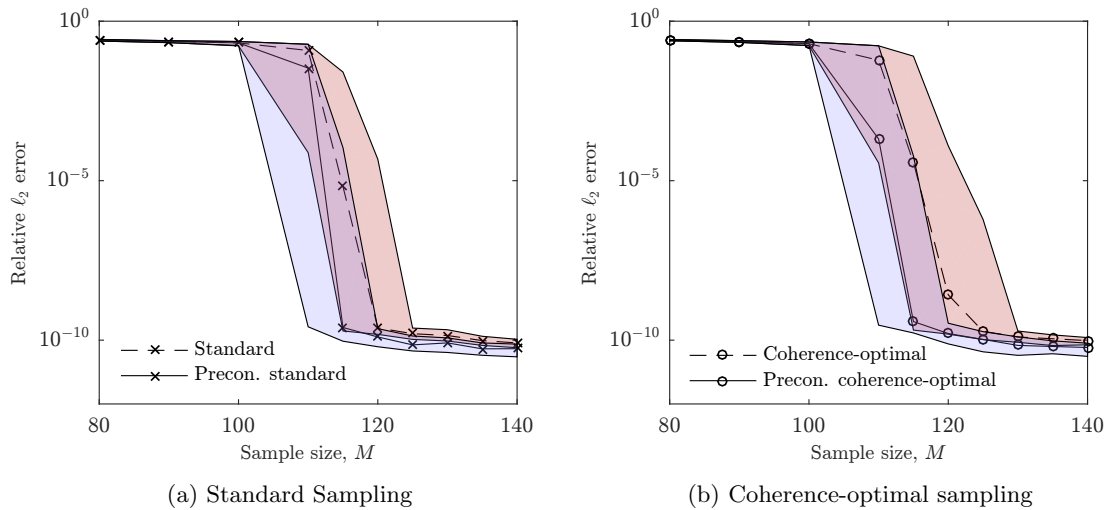


Figure 4: Comparison of relative ℓ_2 error with and without preconditioning for high-dimensional low-order manufactured PCE of Eq. 32 using: (a) standard sampling, (b) coherence-optimal sampling

Accuracy improvements observed in Figures 3 and 4 are direct results of improving the incoherence properties of measurement matrix. To demonstrate these improvements, Figures 5a and 5b compare the median of mutual-coherence of (equivalent) measurement matrix for all four approaches for low-dimensional high-order problem and high-dimensional low-order problem, respectively. It can be seen that for low-dimensional high-order problem, coherence-optimal sampling improves mutual-coherence more significantly than preconditioning alone. However, combination of coherence-optimal sampling and preconditioning leads to the smallest mutual-coherence. For high-dimensional low-order problem, it can be seen that coherence-optimal sampling slightly improves mutual-coherence, while on the other hand, the preconditioning scheme significantly improves the mutual-coherence.

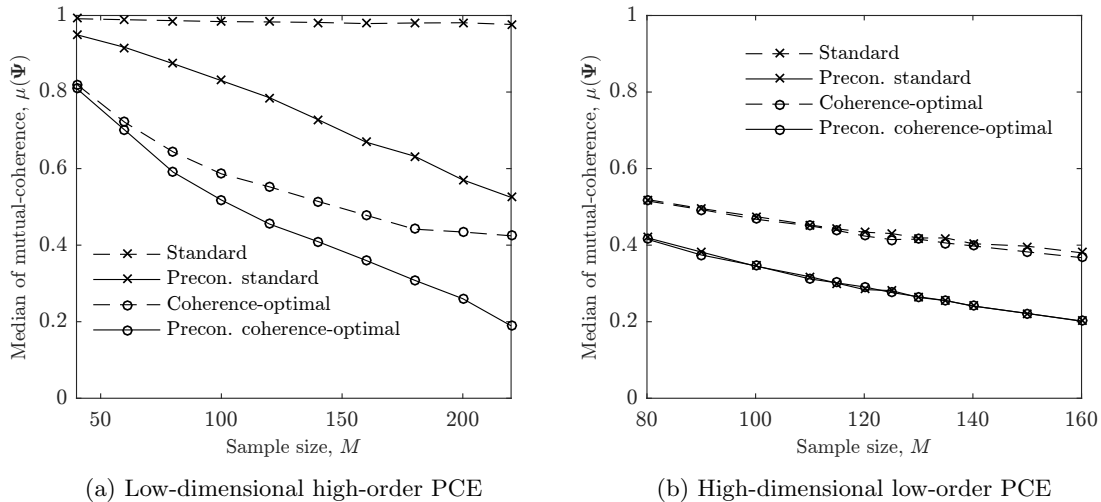


Figure 5: Comparison of mutual-coherence of measurement matrix with and without preconditioning for standard and coherence-optimal sampling for (a) low-dimensional high-order manufactured PCE of Eq. 31 (b) high-dimensional low-order manufactured PCE of Eq. 32

4.3. An approximately sparse function

In this section, we consider the response of a mass-spring system as an approximately sparse target function. In particular, we consider the stochastic mass-spring problem, given by

$$m \frac{d^2 x}{dt^2}(t, \Xi) + \gamma x = f \sin(\omega t), \quad (33)$$

subject to initial conditions

$$x(0) = 0, \quad \dot{x}(0) = 0.$$

We consider the mass m , spring constant γ and frequency ω to be uncertain. We define $\Xi = (m, \gamma, \omega)$, where $m \in [0.018, 0.022]$, $\gamma \in [0.045, 0.035]$ and $\omega \in [1.01, 0.99]$. We choose $x(t = 20)$ to be our QoI and use a 10th-order Legendre polynomial expansion to approximate the QoI. We employ standard sampling approach with and without preconditioning to estimate the coefficients of expansion, and use the analytical solution of Equation 33 as the target function. To compare the performance of standard sampling with and without preconditioning on this target function, the numerical results were obtained under a setting similar to that in the previous example with 100 independent runs. The cardinality of basis set is 286 and we aim to recover the vector of coefficients using a small set of samples. Figure 6 compares the relative error for the QoI of the mass-spring problem with and without preconditioning. It can be seen that approximation accuracy can be significantly improved using preconditioning.

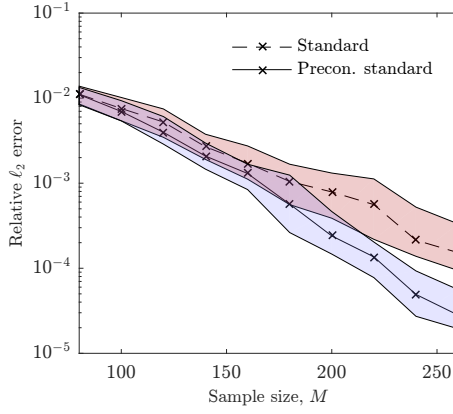


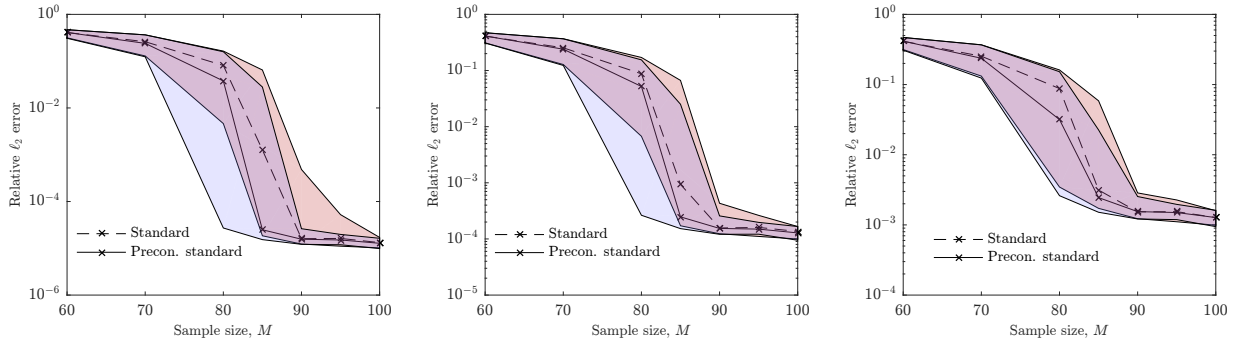
Figure 6: Comparison of relative ℓ_2 errors for sparse recovery of response with and without preconditioning for the stochastic mass-spring problem

4.4. An exactly sparse function with noisy measurement

In all the previous examples, measurements were noiseless. Here, we consider the measurements to be noisy in a problem with a “moderate” combination of dimension and order. Specifically, consider the following 6-dimensional 4th-order generalized Rosenbrock function with random inputs following a uniform density on $[-1, 1]^6$,

$$u(\Xi) = \sum_{i=1}^5 100(\Xi_{i+1} - \Xi_i^2)^2 + (1 - \Xi_i)^2. \quad (34)$$

We consider the measurement noise to follow a normal distribution with zero mean. For a better understanding of accuracy improvement, we consider three different standard deviations for the measurement noise: 10^{-3} , 10^{-2} , and 10^{-1} . Our objective is to recover the sparse vector of coefficients using a sample set whose size is smaller than the cardinality of basis set which is 210. We report the results for 100 independent trials for standard sampling with and without preconditioning. It can be seen in Figure 7 that preconditioning significantly improves the approximation accuracy for standard sampling when the standard deviation of noise is relatively small. On the other hand, when standard deviation of noise is relatively large, it is more likely that the preconditioning matrix undesirably amplifies the noise vector. In this case, we observed that the cross-validation algorithm typically identified a larger λ value, which limited the accuracy improvement that can be achieved by preconditioning.



(a) Measurement noise $\sim N(0, 10^{-3})$ (b) Measurement noise $\sim N(0, 10^{-2})$ (c) Measurement noise $\sim N(0, 10^{-1})$

Figure 7: Comparison of relative errors in recovering the Rosenbrock function with noisy measurements by compressive sampling (using standard samples) with and without preconditioning.

5. Conclusion

In this work, we introduced a preconditioning approach to improve the accuracy of compressive sampling-based recovery of polynomial chaos expansions. We demonstrated the potential accuracy improvement offered

solely by preconditioning a measurement matrix that has already been formed, e.g. in cases where samples are already collected. To do this, we multiply both sides of the equation system by a preconditioning matrix. The preconditioning matrix is designed such that the preconditioned measurement matrix has better incoherence properties and signal-to-noise ratio for the preconditioned problem is not undesirably large, thereby enhancing the recovery accuracy. We provided theoretical motivation for such scheme along with various numerical examples to validate the preconditioning approach.

6. References

References

- [1] P. R. Conrad, Y. M. Marzouk, Adaptive smolyak pseudospectral approximations, *SIAM Journal on Scientific Computing* 35 (6) (2013) A2643–A2670.
- [2] P. G. Constantine, M. S. Eldred, E. T. Phipps, Sparse pseudospectral approximation method, *Computer Methods in Applied Mechanics and Engineering* 229 (2012) 1–12.
- [3] V. Barthelmann, E. Novak, K. Ritter, High dimensional polynomial interpolation on sparse grids, *Advances in Computational Mathematics* 12 (4) (2000) 273–288.
- [4] G. T. Buzzard, Global sensitivity analysis using sparse grid interpolation and polynomial chaos, *Reliability Engineering & System Safety* 107 (2012) 82–89.
- [5] Y. Shin, D. Xiu, Nonadaptive quasi-optimal points selection for least squares linear regression, *SIAM Journal on Scientific Computing* 38 (1) (2016) A385–A411.
- [6] J. Hampton, A. Doostan, Coherence motivated sampling and convergence analysis of least squares polynomial chaos regression, *Computer Methods in Applied Mechanics and Engineering* 290 (2015) 73–97.
- [7] A. Doostan, H. Owhadi, A non-adapted sparse approximation of PDEs with stochastic inputs, *Journal of Computational Physics* 230 (8) (2011) 3015–3034.
- [8] L. Guo, A. Narayan, T. Zhou, Y. Chen, Stochastic collocation methods via ℓ_1 minimization using randomized quadratures, *SIAM Journal on Scientific Computing* 39 (1) (2017) A333–A359.
- [9] L. Yan, L. Guo, D. Xiu, Stochastic collocation algorithms using ℓ_1 minimization, *International Journal for Uncertainty Quantification* 2 (3).
- [10] N. Alemazkoo, H. Meidani, A near-optimal sampling strategy for sparse recovery of polynomial chaos expansions, *arXiv preprint arXiv:1702.07830*.
- [11] J. Peng, J. Hampton, A. Doostan, A weighted ℓ_1 -minimization approach for sparse polynomial chaos expansions, *Journal of Computational Physics* 267 (2014) 92–111.
- [12] L. Yan, Y. Shin, D. Xiu, Sparse approximation using ℓ_{1-2} minimization and its application to stochastic collocation, *SIAM Journal on Scientific Computing* 39 (1) (2017) A229–A254.
- [13] H. Rauhut, R. Ward, Sparse Legendre expansions via ℓ_1 -minimization, *Journal of approximation theory* 164 (5) (2012) 517–533.
- [14] G. Tang, G. Iaccarino, Subsampled Gauss quadrature nodes for estimating polynomial chaos expansions, *SIAM/ASA Journal on Uncertainty Quantification* 2 (1) (2014) 423–443.
- [15] J. Hampton, A. Doostan, Compressive sampling of polynomial chaos expansions: convergence analysis and sampling strategies, *Journal of Computational Physics* 280 (2015) 363–386.
- [16] J. D. Jakeman, A. Narayan, T. Zhou, A generalized sampling and preconditioning scheme for sparse approximation of polynomial chaos expansions, *SIAM Journal on Scientific Computing* 39 (3) (2017) A1114–A1144.
- [17] V. Abolghasemi, S. Ferdowsi, S. Sanei, A gradient-based alternating minimization approach for optimization of the measurement matrix in compressive sensing, *Signal Processing* 92 (4) (2012) 999–1009.

- [18] G. Li, Z. Zhu, D. Yang, L. Chang, H. Bai, On projection matrix optimization for compressive sensing systems, *IEEE Transactions on Signal Processing* 61 (11) (2013) 2887–2898.
- [19] D. Xiu, Numerical methods for stochastic computations: a spectral method approach, Princeton University Press, 2010.
- [20] H.-J. Bungartz, M. Griebel, Sparse grids, *Acta numerica* 13 (2004) 147–269.
- [21] Y. Shin, D. Xiu, On a near optimal sampling strategy for least squares polynomial regression, *Journal of Computational Physics* 326 (2016) 931–946.
- [22] J. H. Ender, On compressive sensing applied to radar, *Signal Processing* 90 (5) (2010) 1402–1414.
- [23] J. F. Gemmeke, H. Van Hamme, B. Cranen, L. Boves, Compressive sensing for missing data imputation in noise robust speech recognition, *Selected Topics in Signal Processing, IEEE Journal of* 4 (2) (2010) 272–287.
- [24] M. Lustig, D. Donoho, J. M. Pauly, Sparse MRI: The application of compressed sensing for rapid MR imaging, *Magnetic resonance in medicine* 58 (6) (2007) 1182–1195.
- [25] E. J. Candes, J. K. Romberg, T. Tao, Stable signal recovery from incomplete and inaccurate measurements, *Communications on pure and applied mathematics* 59 (8) (2006) 1207–1223.
- [26] S. S. Chen, D. L. Donoho, M. A. Saunders, Atomic decomposition by basis pursuit, *SIAM review* 43 (1) (2001) 129–159.
- [27] R. Tibshirani, Regression shrinkage and selection via the lasso, *Journal of the Royal Statistical Society. Series B (Methodological)* (1996) 267–288.
- [28] R. Tibshirani, Regression shrinkage and selection via the lasso: a retrospective, *Journal of the Royal Statistical Society: Series B (Statistical Methodology)* 73 (3) (2011) 273–282.
- [29] P. Yin, Y. Lou, Q. He, J. Xin, Minimization of ℓ_{1-2} for compressed sensing, *SIAM Journal on Scientific Computing* 37 (1) (2015) A536–A563.
- [30] Z. Xu, H. Zhang, Y. Wang, X. Chang, Y. Liang, $\ell_{1/2}$ regularization, *Science China Information Sciences* 53 (6) (2010) 1159–1169.
- [31] E. J. Candès, The restricted isometry property and its implications for compressed sensing, *Comptes Rendus Mathématique* 346 (9) (2008) 589–592.
- [32] H. Rauhut, Compressive sensing and structured random matrices, *Theoretical foundations and numerical methods for sparse recovery* 9 (2010) 1–92.
- [33] D. L. Donoho, M. Elad, V. N. Temlyakov, Stable recovery of sparse overcomplete representations in the presence of noise, *Information Theory, IEEE Transactions on* 52 (1) (2006) 6–18.
- [34] M. Elad, Sparse and redundant representations: From theory to applications in signal and image processing.
- [35] M. Elad, Optimized projections for compressed sensing, *IEEE Transactions on Signal Processing* 55 (12) (2007) 5695–5702.
- [36] L. Zelnik-Manor, K. Rosenblum, Y. C. Eldar, Sensing matrix optimization for block-sparse decoding, *IEEE Transactions on Signal Processing* 59 (9) (2011) 4300–4312.
- [37] S. Tian, X. Fan, Z. Li, T. Pan, Y. Choi, H. Sekiya, Orthogonal-gradient measurement matrix construction algorithm, *Chinese Journal of Electronics* 25 (1) (2016) 81–87.
- [38] T. Hong, H. Bai, S. Li, Z. Zhu, An efficient algorithm for designing projection matrix in compressive sensing based on alternating optimization, *Signal Processing* 125 (2016) 9–20.
- [39] G. Li, X. Li, S. Li, H. Bai, Q. Jiang, X. He, Designing robust sensing matrix for image compression, *IEEE Transactions on Image Processing* 24 (12) (2015) 5389–5400.

- [40] T. Hong, Z. Zhu, An efficient method for robust projection matrix design, *Signal Processing* 143 (2018) 200–210.
- [41] E. Van Den Berg, M. Friedlander, *SPGL1: A solver for large-scale sparse reconstruction* (2007).
- [42] M. Schmidt, *minfunc: unconstrained differentiable multivariate optimization in matlab* (2006).
- [43] D. L. Donoho, J. Tanner, Neighborliness of randomly projected simplices in high dimensions, *Proceedings of the National Academy of Sciences of the United States of America* 102 (27) (2005) 9452–9457.
- [44] D. L. Donoho, J. Tanner, Precise undersampling theorems, *Proceedings of the IEEE* 98 (6) (2010) 913–924.